CO$_2$ Gasification of torrefied wood. A kinetic study.

Liang Wang,[†] Gábor Várhegyi,[,‡] and Øyvind Skreiberg[†]*

[†]SINTEF Energy Research, Postboks 4761 Sluppen, NO-7465 Trondheim, Norway

[‡]Institute of Materials and Environmental Chemistry, Research Centre for Natural Sciences, Hungarian Academy of Sciences, PO Box 286, Budapest, Hungary 1519

KEYWORDS: Torrefied wood; birch; spruce; thermogravimetry; gasification; kinetics.

ABSTRACT

The CO$_2$ gasification of torrefied wood samples was examined by thermogravimetry (TGA) at linear, modulated and constant reaction rate (CRR) temperature programs. The untreated raw materials and chars prepared at 750°C were also included in the study. The gasification temperature range separated sufficiently from the pyrolysis in the experiments for its separate analysis. Characteristic gasification reactivity differences were observed between the samples that were due to the differences of the char-forming reactions at different conditions. Various groups of experiments were evaluated together by the method of least squares, under various hypotheses on the dependence of the reaction rate on the reacted fractions. The differences between the samples were described by different pre-exponential factors while the rest of the kinetic parameters were kept identical during an evaluation. The effect of thermal annealing on the gasification kinetics was also expressed by the values of the pre-exponential factors. When the experiments of the samples prepared from birch were evaluated together, self-accelerating kinetics was obtained with E=225kJ/mol. The experiments belonging to the samples prepared from spruce resulted in n-order kinetics with E=223kJ/mol.

1. INTRODUCTION

The increased use of biomass as a renewable energy source is an important way to reduce the CO$_2$ emission of the energy production. However, the widespread use of biomass fuels is frequently hindered by their unfavorable fuel characteristics like high moisture content, poor grindability, low calorific value and low bulk density. Torrefaction is one of the potential solutions to these problems. It results in improved biomass fuel

properties such as reduced moisture content, improved hydrophobic behavior, better storability, and less energy consumption during grinding.[1-2] Torrefaction is typically conducted at 200–300°C, at atmospheric pressure, in the absence of oxygen. The lignocellulosic biomass is partly decomposed during the torrefaction releasing condensable liquids and non-condensable gases into the gas phase.[3] Primarily the xylan-containing hemicellulose polymers decompose because they are the most reactive polymer structures in biomass.[4-7] The extractives of the biomass also decompose while the cellulose and lignin are moderately impacted during torrefaction, depending on the feedstock composition and the torrefaction temperature.[8,9] The torrefaction, as a pretreatment, is advantageous for the biomass gasification, too. Prins et al. showed that torrefaction reduces the thermodynamic losses of the wood gasification by oxygen.[10] Besides, the usual advantages of the torrefied woods, like better grindability, reduced moisture content and greater heating value may also be beneficial in the various gasification processes. Svoboda et al. compared various biomass pretreatment methods for entrained-flow gasification and emphasized the advantages of torrefaction, which included a smooth feeding for the reactor, and the favorable properties for the storage of the raw material.[11]

The CO_2 gasification is a promising possibility for the utilization of biomass materials either as a stand-alone procedure or as a partial process of a more complex gasification. In the latter case the char and the CO_2 are formed during a partial oxidation of the feedstock and reacts further at temperatures above 800°C. There are several studies on CO_2 gasification kinetics of woody biomass chars at various operating conditions and with different char preparation methods. A major part of the existing knowledge on the kinetics of CO_2 gasification of biomass chars is summarized in the extensive review of Di Blasi.[12] A recent general review is also available,[13] while a related field, the CO_2 gasification of coals, was surveyed in details in 2011.[14] However, the properties of the torrefied woods differ significantly from their raw materials in several respects,[6,7,15] and the chars formed from torrefied woods also differ from the chars produced directly from their feedstocks.[16,17] Hence, there is a need for research on the gasification of torrefied woods.

The present work aimed at studying the kinetics of the CO_2 gasification of torrefied wood under kinetic control. We are not aware of any study on this particular topic in the literature, though the effect of torrefaction on the CO_2 gasification of a grass, *Miscanthus × giganteus*, was examined in details in a recent work.[18] Besides, Marcilla et al. studied the effect of the heating profiles of the charcoal formation on the reactivity to CO_2 of almond shells.[16] In this latter work the lower temperature part of the heating included typical torrefaction conditions which were followed by fast heating to 850°C. The gasification reactivity was characterized by the isothermal reaction rate of the char+CO_2 reaction at 800°C.

Due to its high precision and well-controlled experimental conditions, TGA is a useful tool for studying gasification in the kinetic regime. If the reaction is far from the equilibrium, then the kinetics usually can be well described by the following type of equations:[12]

$d\alpha/dt = A \exp(-E/RT) f(\alpha)$ (1)

where A is the pre-exponential factor, α is the reacted fraction predicted by the kinetic model, and function $f(\alpha)$ approximates the reactivity change of the sample as the gasification proceeds. A obviously depends on

the partial pressure of the CO_2. In the present study the A values belong to pure CO_2 at atmospheric pressure, i.e. $P_{CO_2}=101.3$kPa.

The work includes a comparison with gasification of the untreated woods as well as that of chars prepared at 750°C. Besides, the dependence of the results on the temperature programs of the gasification was also studied. A particular care was taken to determine reliable kinetic data based on the simultaneous least squares evaluation of experiments with different temperature programs.

2. SAMPLES AND METHODS

2.1 Samples. Birch and spruce samples were taken from standard Norwegian construction boards. The samples were torrefied as described by Tapasvi et al.[19] In the present work the birch and spruce samples torrefied at 225 and 275°C for 60 minutes as 10×10×10mm cubes were studied. The notation of the samples refer to the type of wood (B for birch and S for spruce), followed by the torrefaction temperature. Hence the torrefied samples are denoted as B225, S225, B275 and S275. Table 1 shows the ultimate and proximate analyses and the higher heating values of the untreated and torrefied samples.

For a comparison, the behavior of the original raw materials (untreated woods) and chars prepared at 750°C in a TGA were also included in the studies. These samples are denoted as B---, S---, B750 and S750, respectively. Chars B750 and S750 were prepared at 20 °C/min heating rate with a 10 min holding time at the final temperature of 750°C.

Before the experiments, the samples were cut into smaller pieces and ground in a cutting mill that was equipped with a 1 mm bottom sieve. The samples were sieved afterward and the particles in the range of 63-125 μm were used for the kinetic study.

Table 1: Proximate and ultimate analyses of the untreated and torrefied woods[a]

Sample	Proximate analysis[b]			Ultimate analysis[b]					HHV[c]
	VM	fC	Ash	C	H	O	N	S	
B---	89.4	10.4	0.2	48.62	6.34	44.90	0.09	< 0.05	19.80
B225	86.4	13.2	0.4	49.90	5.98	43.97	0.10	< 0.05	19.90
B275	77.7	21.9	0.4	54.16	5.65	40.02	0.12	0.05	21.40
S---	86.3	13.4	0.2	50.10	6.36	43.52	0.07	< 0.05	20.45
S225	84.0	15.8	0.2	50.97	6.15	42.76	0.07	< 0.05	20.62
S275	75.7	24.2	0.2	55.33	5.73	38.80	0.09	0.05	22.05

[a] From the work of Tapasvi et al.[20] which studied the oxidation kinetics of the samples listed.
[b] % (m/m), dry basis. [c] Higher heating value, MJ/kg, dry basis.

2.2 Experimental Setup and Procedure. The experiments were carried out by a Q5000 IR TG analyzer from TA Instruments which has a sensitivity of 0.1 μg. High purity CO_2 was used as purge gas with a gas flow of 150 mL/min. Three different temperature programs were employed: linear T(t) with a heating rate of 20°C/min; modulated experiments where a sine function with 5°C peak amplitude and 200 s wavelength was added to a 5°C/min linear T(t); and constant heating rate (CRR) T(t). The modulated experiments served to increase the rather limited kinetic information content of the linear T(t) experiments. In the "constant reaction rate" (CRR) experiments the equipment regulated the heating of the samples so that the reaction rate would remain below a preset limit.[21] The domain of the gasification started around 650–700°C and terminated below 1000°C. The T(t) functions of the CRR experiments are usually irregular;[20] the mean *dT/dt* in the domain of gasification varied between 2.5 and 4.4°C/min.

Due to the high heat demand of the $C+CO_2=2CO$ reaction, the initial sample mass of the TGA experiments were chosen so that heat transfer would not be a rate determining factor. Based on earlier experience,[22] the initial sample mass of the two charcoal samples, B750 and S750 was around 1.2 mg at 20°C/min and around 4.4 mg in the experiments with slower heating. Higher amounts were used for the untreated and torrefied wood samples, because most of the mass of these samples was lost in the devolatilization reactions prior to their gasification. In this way the highest mass loss rate varied between 1 and 5 μg/s in the temperature domain of gasification. Figures illustrating the repeatability of the experiments can be found in the Supporting Information.

Two sorts of experiments were carried out to check the effect of the heating rate below 700°C: (i) slow heating of 2°C/min; (ii) the highest heating rate permitted by the equipment. In both cases the temperature program continued with a regular 20°C/min heating above 700°C, as outlined in the Results and Discussion section. The setting of the highest heating rate resulted in heating rates around 1400°C/min at the thermocouple sensor connected to the sample holder. To avoid possible overruns, this fast heating was stopped at two short isothermal sections (5 min at 690°C and 3 min at 700°C).

2.3. Kinetic Evaluation by the Method of Least Squares and Characterization of the Fit Quality.
Fortran 95 and C++ programs were used for the numerical calculations and for graphics handling, respectively. The employed numerical methods have been described in details earlier.[23] The kinetic evaluation was based on the least squares evaluation of the *-dm^obs/dt* curves, where *m^obs* is the sample mass normalized by the initial dry sample mass. The method used for the determination of *-dm^obs/dt* does not introduce considerable systematic errors into the least squares kinetic evaluation of experimental results.[24] The model was solved numerically along the empirical temperature – time functions. The minimization of the least squares sum was carried out by a direct search method, as described earlier.[23] Such values were searched for the unknown model parameters that minimized the following objective function (*of*):

$$of = \sum_{k=1}^{N} \sum_{i=1}^{N_{points}} \frac{\left[\left(\frac{dm}{dt}\right)_k^{obs}(t_i) - \left(\frac{dm}{dt}\right)_k^{calc}(t_i)\right]^2}{N_{points} h_k^2} \tag{2}$$

Here N is the number of experiments evaluated together. N varied between 3 and 16 in the present work, as explained in Section 3.2. N_{points} denotes the number of t_i time points on a given curve and m is the sample mass normalized by the initial dry sample mass. The division by h_k^2 served to counterbalance the high magnitude differences. h_k was chosen to be the highest observed value of the given experiment:

$$h_k = \max \left(\frac{dm}{dt} \right)_k^{obs} \qquad (3)$$

The normalization by the highest observed values in the least squares sum assumes implicitly that the relative precision is roughly the same for the different experiments. This assumption has proved to be useful in numerous works on non-isothermal kinetics since 1993.[25]

The obtained fit quality can be characterized separately for each of the experiments evaluated together. For this purpose the relative deviation ($reldev$, %) was used. The root mean square difference between the observed and calculated values is expressed as percent of peak maximum. For experiment k we get:

$$reldev\,(\%) = 100 \left\{ \sum_{i=1}^{N_{points}} \frac{\left[\left(\frac{dm}{dt}\right)_k^{obs}(t_i) - \left(\frac{dm}{dt}\right)_k^{calc}(t_i) \right]^2}{N_{points} h_k^2} \right\}^{0.5} \qquad (4)$$

The fit quality for a given group of experiments was characterized by the root mean square of the corresponding relative deviations. The relative deviation of N experiments evaluated together can be expressed by equations $2 - 4$ as

$$reldev_N\,(\%) = 100 \sqrt{of} \qquad (5)$$

Obviously a smaller $reldev_N$ value indicates a better fit for the given group of experiments.

3. RESULTS AND DISCUSSION

3.1. Effects of the Pyrolysis Conditions on the Gasification. Figure 1 shows the DTG curves of four samples from 150 to 1000°C at a constant heating rate of 20°C/min. One can see the usual pyrolysis reactions with peak tops around 400°C. The "shoulder" of the peaks observable for the untreated woods is due to the partly overlapping hemicellulose and cellulose decompositions. This shoulder was absent in samples B275 and S275 because the hemicelluloses wholly decompose during the torrefaction at 275°C.[9] The presence of CO_2 did not result in noticeable effects on the DTG curves of the pyrolysis reactions. Above 700°C the rate of the decomposition reactions becomes negligible and the gasification reaction dominates.
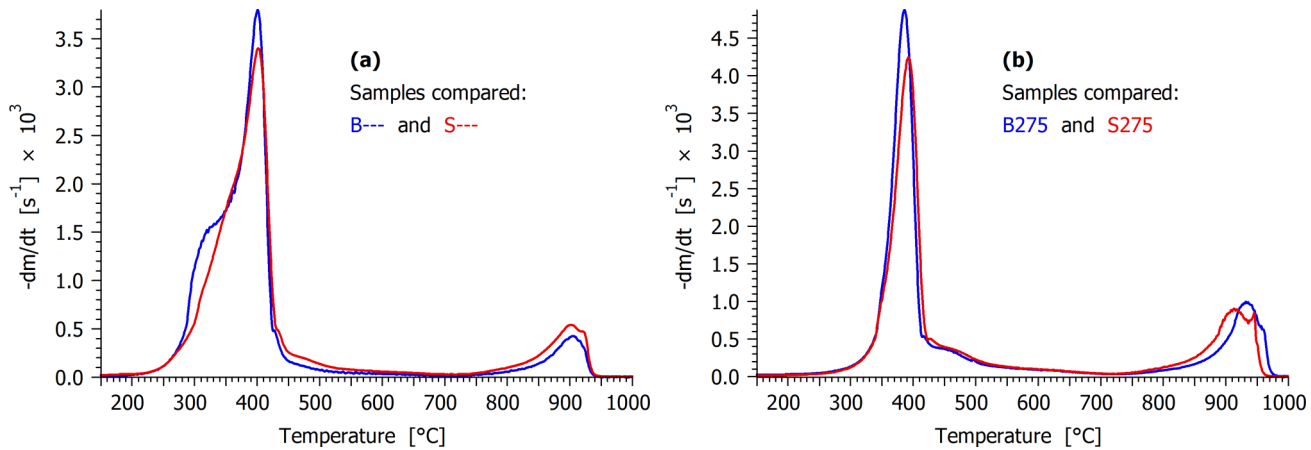
Figure 1. Comparison of the DTG curves of the two untreated woods, B--- and S--- **(a)**; and the two samples torrefied at 275°C, B275 and S275 **(b)**, at 20°C/min heating rate.

Figure 2 exhibits the DTG curves of all examined samples from 720 to 1000°C at 20°C/min. In the case of the birch samples, the solid residue of the untreated wood (green curve) gasified at the lowest temperature. It was followed by the torrefied woods prepared at 225 and 275°C (blue and red curves) while the char prepared at 750°C in a TGA (black curve) gasified at the highest temperature. The order of the curves was the same for the samples prepared from spruce, though, in that case the curve of sample S225 was very close to that of S--- and the curve of sample S750 was very close to that of S275.

It is interesting to observe that the peaks of –dm/dt have similar shape and width for the birch samples in Figure 2a, and the peaks of the spruce samples are also similar to each other in Figure 2b. See the Supporting Information for more plots reflecting these similarities. Under such circumstances the reactivity of a sample can be characterized by the position of the peak at a given heating rate: the more reactive a sample is the lower is the temperature of its peak. The position of the gasification peaks can be characterized by the temperature of the half mass-loss of the gasification, T_{half} (°C). T_{half} is more suitable for our purposes than the temperature of the peak top, because the latter, connected to a single point of the curve, is influenced by the peculiarities of the peak shape and is more sensitive to experimental noise.
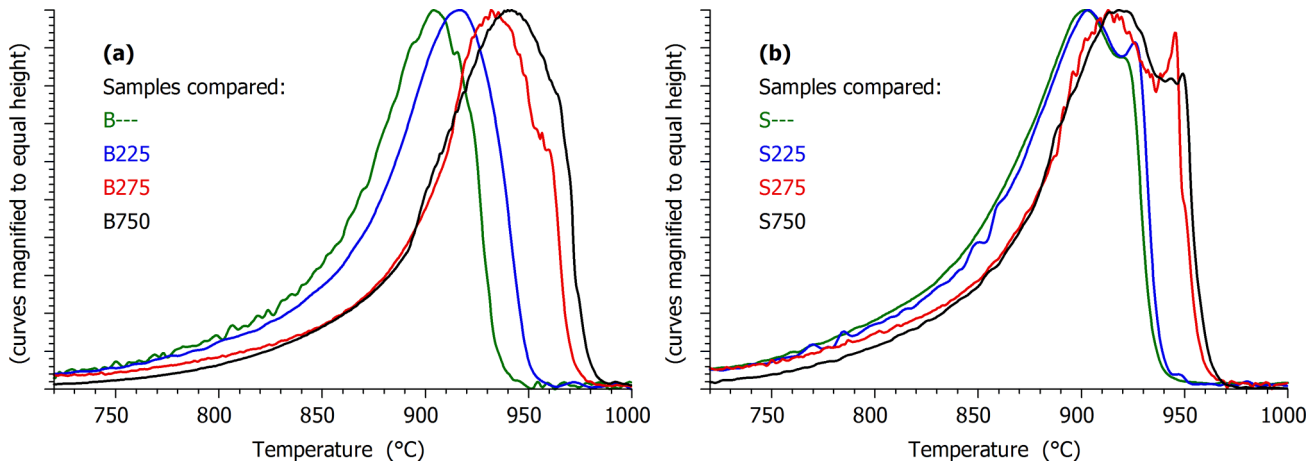
Figure 2. Comparison of the DTG curves of the birch samples **(a)**; and the spruce samples **(b)**, at 20°C/min heating rate, in the temperature domain of the gasification.

Note that all samples decomposed to char till the start of the gasification domain, hence Figure 2 compares the behavior of chars formed from exactly the same raw materials in different ways. Hence the differences shown in Figures 2a and 2b should be connected to the pyrolysis conditions. To examine this in more detail, TGA experiments were carried out with low (2°C/min), and high (ca. 1400°C/min) heating rates in the domain of devolatilization. The heating was continued by a usual 20°C/min heating above 700°C. The results are summarized in Table 2.

Table 2: The temperatures belonging to the half mass loss of the gasification (T_{half}, °C) at 20°C/min heating rate

Sample	Heating rate below 690°C		
	2°C/min[a]	20°C/min	~1400°C/min[a]
B---	889	889	878
B225	–	900	–
B275	921	922	926
B750	–	927	–
S---	887	886	873
S225	–	890	–
S275	904	904	904
S750	–	906	–

[a] The experiments with 2 and ca. 1400°C/min heating rates below 690°C served to clarify the role of the pyrolysis conditions, as described in the text.

The column of 20°C/min in the pyrolysis domain gives a quantitative measure to the effects shown by Figure 2. The values in columns 2°C/min and 20°C/min are practically identical indicating that an extra slow heating in the pyrolysis domain had only small effects on the gasification. The fast heating rate in the pyrolysis domain had a mentionable effect for the untreated woods; T_{half} decreased by 11 and 13°C. (Obviously a lower T_{half} value indicates a higher reactivity at a given heating rate.) The fast heating rate had only small effects on the reactivity of torrefied samples B275 and S275. See the corresponding figures in the Supporting Information.

On the other hand, the torrefaction can result in a higher change in the reactivity. In the case of the birch wood, even the 225°C torrefaction resulted in a mentionable decrease in the reactivity: it increased T_{half} by 11°C. The difference was higher at B275, its T_{half} was 33°C higher than that of the untreated birch. The corresponding differences were lower in the case of the spruce samples, though T_{half} of S275 was still higher than that of the untreated spruce by 18°C.

The above observations can be connected to the fate of the tars during the gasification. The sample mass was very low in the TGA experiments, the samples were spread in a thin layer and the gas flow is high. One can assume that most of the formed tars quickly leave the surfaces of the forming char. That explains why pyrolysis at 2°C/min and 20°C/min heating rates resulted in the same reactivity. The fast heating rate of ~1400°C/min had small effect on samples B275 and S275, and a moderate effect on the untreated woods.

The tar has more opportunity for secondary reactions in the 10×10×10 mm cubes used for the torrefaction. That may explain the considerable reactivity differences between the untreated woods and the woods torrefied at 275°C. Note that the secondary reactions of the tars have a high importance in the charcoal production: more char is formed if the tars are kept in the hot charcoal zone due to secondary char forming reactions.[26,27] The lower reactivity of chars B750 and S750 may be due to thermal annealing[12] during their preparation, and during their repeated heating in the TGA experiments, as discussed in Section 3.5.

3.2. Kinetic Evaluation of the Experiments. Eq 1 in the Introduction shows the family of models considered. It describes the change of the reacted fraction at any T(t). The reacted fraction predicted by the kinetic model has a linear relationship with the predicted sample mass, m^{calc}:

$$\alpha(t) = \frac{1-m^{calc}(t)}{1-m^{calc}(\infty)} = c[1 - m^{calc}(t)] \tag{6a}$$

$$-dm^{calc}/dt = c \, d\alpha/dt \tag{6b}$$

Note that the experimental counterpart of $\alpha(t)$ cannot be read from the TGA curves in a reliable way, because the start and end temperatures of the gasification is not exactly defined. (The start of the gasification overlaps with the slow carbonization of the chars, which is the last step of the devolatilization, while the end of the gasification overlaps with the decomposition of the carbonates formed from the mineral matter of the chars in the presence of CO_2). Accordingly the non-linear method of least squares is employed, as described in section 2.3, and the parameter c is determined together with the kinetic parameters during the evaluation of the experiments.

The $f(\alpha)$ function of eq 1 can be deduced from theories in the case of idealized, homogeneous carbon particles. If the reaction takes place on the external surface of homogeneous, isotropic spherical particles of equal size, then the contracting sphere (shrinking sphere) model can be employed, while the presence of internal reaction surfaces leads to self-acceleration which can be described by random-pore models.[28-30] The biomass chars, however, are usually too complex for these theories because they are chemically inhomogeneous, geometrically irregular, and contain mineral matter with more or less catalytic activity. Accordingly, only empirical $f(\alpha)$ functions can be employed. If $f(\alpha)$ is a monotonically decreasing function (i.e. if no self-acceleration can be observed) then it is usually approximated by n-order kinetics:

$$f(\alpha) = (1-\alpha)^n \tag{7}$$

Here n is an empirical parameter. In more complex cases an empirical formula may be used that can mimic a wide varieties of shapes[31]

$$f(\alpha) \cong normfactor \, (\alpha+z)^a \, (1-\alpha)^n \tag{8}$$

Here $n>0$, $a \geq 0$ and $z>0$ are adjustable model parameters that define the shape of $f(\alpha)$ and *normfactor* ensures that max $f=1$. (The normalization of $f(\alpha)$ is required for the unambiguity of eq 1. *normfactor* is a simple function of parameters n, a and z.[31])

When $a=0$, eq 8 reduces to the n-order kinetics (eq 7). At $a=1$ we get a slightly simpler relationship which contain only two unknown parameters, n and z:[9,20]

$$f(\alpha) \cong normfactor \, (\alpha+z) \, (1-\alpha)^n \tag{9}$$

Eq 9 can describe monotonically decreasing $f(\alpha)$ functions as well as curves having a maximum, as shown in the next section.

In the present work the applicability of the above three $f(\alpha)$ approximations (equations 7, 8 and 9) were tested on the gasification of each sample. However, the fit quality obtained by equations 8 and 9 was similar, hence the results by eq 8 will not be presented. (Eq 9 was selected for the presentation because it is simpler and contains less unknown parameters than eq 8.)

The available experiments for a given sample were evaluated together. E and the parameters of the $f(\alpha)$ function were common parameters for the experiments evaluated together, while each experiment had its own pre-exponential factor and c parameter. In this way 3 to 5 experiments were evaluated together for a sample. In another attempt all samples of a given wood were evaluated together assuming common E and $f(\alpha)$. In this case the number of the experiments evaluated together, N, was 16. The advantage of this latter approach is the obtaining of kinetics valid for a wider range of samples. It was hoped that common characteristics of the samples prepared from birch and spruce, respective, could be found in that way.

3.3. Results of the Kinetic Evaluation. Table 3 summarizes the evaluations with n-order kinetics as well as by the application of eq 9. This latter is called nz-kinetics in the table and in the treatment that follows.

When the n-order kinetics and the nz-kinetics gave similar fit qualities, the n-order kinetics was preferred because it has simpler form and less unknown parameters. In the first 5 rows of the table, from sample B--- till sample S---, the nz-kinetics was accepted because it gave considerably better fit quality (smaller $reldev_N$ value) than the corresponding evaluations by the n-order model. n-order kinetics was accepted in the rest of the evaluations, from sample S225 till the joint evaluation of the spruce experiments.

Figure 3 displays the obtained $f(\alpha)$ curves. Four of the birch evaluations resulted in curves having a maximum between α=0.38–0.45, where the lowest value, α=0.38 belong to the common evaluation of the birch samples. These curves show some similarity to the $f(\alpha)$ curves deduced from random pore models.[30] The self-accelerating period at the beginning of these curves can be due to the gasification in the internal pores. Four spruce evaluations resulted in n-order reactions with n=0.36–0.42. There is no self-acceleration in this case. Nevertheless these curves run above the theoretical contracting sphere $f(\alpha)$ function (n-order kinetics with n=2/3) till the end of the interval, as the gray dashed curve indicates in Fig. 3b. A plausible explanation is the assumption of a more limited role of the internal pores for spruce. The nz-kinetics gave better performance than the n-order kinetics for samples B750 and S---, but the corresponding $f(\alpha)$ functions were monotonically decreasing. (In the case of S--- the monotonicity was not entirely consistent; there is a hardly observable small maximum at the very beginning of the curve, at α=0.04.) Nevertheless, these curves remained above the n-order curves till nearly the end of the domain, indicating that the reaction surface is higher than in the cases predicted by the n-order models. This observation can probably also be due to the contribution of the internal pore surfaces. Note that the difference between the fit qualities of the nz and n-order kinetics was lower here than for samples B---, B225 and B275, as shown in Table 2. The n-order evaluation gave n=0.34 and n=0.35 for samples B750 and S---.

Table 3: The kinetic evaluations carried out and a summary of the results[a]

Samples evaluated	N	n-order kinetics		nz-kinetics		Accepted kinetics	Further characteristics of the accepted version			
		$reldev_N$	E	$reldev_N$	E		average $\log_{10} A$	std. dev $\log_{10} A$	n	z
B---	5	5.2	220.2	2.8	219.6	nz	7.37	0.18	0.51	0.64
B225	3	5.2	225.5	3.1	222.2	nz	7.33	0.11	0.52	0.72
B275	5	6.5	229.1	3.9	224.1	nz	7.29	0.10	0.64	0.40
B750	3	4.2	227.3	3.8	226.7	nz	7.30	0.14	0.43	2.67
all birch samples together	16	5.5	225.5	3.9	225.2	nz	7.43	0.21	0.52	0.81
S---	5	3.8	219.8	3.4	219.1	nz	7.38	0.16	0.44	2.12
S225	3	3.6	225.7	3.7	224.4	n-order	7.60	0.14	0.36	–
S275	5	4.8	224.6	4.7	224.0	n-order	7.50	0.11	0.40	–
S750	3	5.0	226.5	5.5	225.8	n-order	7.53	0.10	0.42	–
all spruce samples together	16	4.5	223.4	4.5	222.7	n-order	7.50	0.16	0.38	–

[a] Each evaluation was carried out by n-order kinetics and by eq 9. This latter is referred as *nz-kinetics*. N is the number of experiments evaluated together. The dimensions of E and A are kJ/mol and s⁻¹. The acceptance was based primarily on the fit quality ($reldev_N$). n-order kinetics was preferred at nearly identical $reldev_N$ values due to its simpler form and fewer parameters.
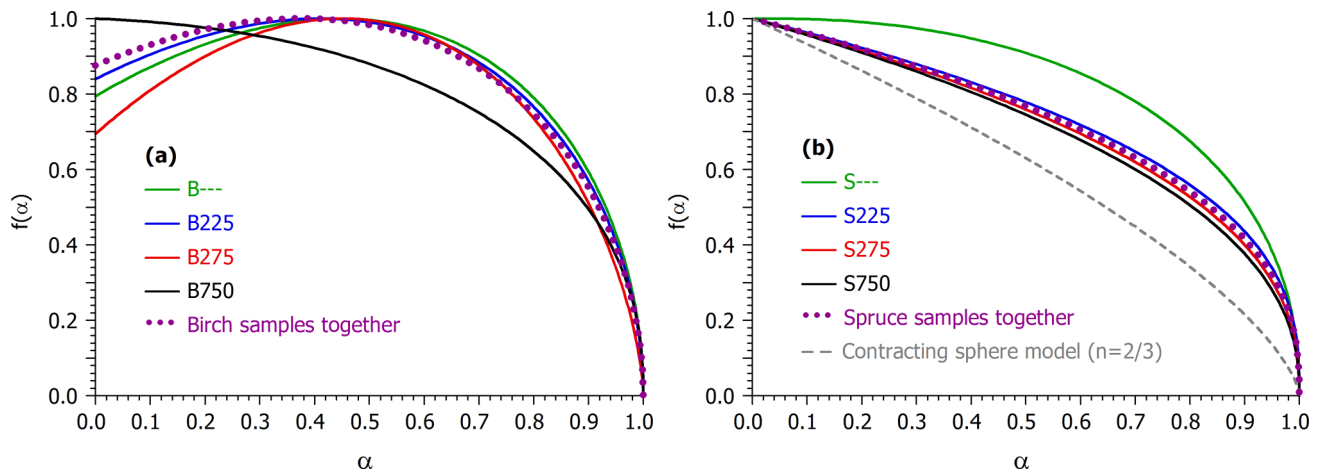

Figure 3. The obtained $f(\alpha)$ functions. (See Table 2.) The contracting sphere model (dashed gray curve in Fig. 3b) is drawn only to help the discussion.

3.4. About the Obtained Activation Energies. The closeness of the obtained E values is a particularly notable feature in Table 3. The average and standard deviations of the 20 E values listed in Table 3 are 224.1 and 2.7 kJ/mol. The averages and standard deviations of the various subgroups of Table 3 are similar. For example, the averaging of the 10 accepted E values results in a mean of 223.7 kJ/mol with a standard deviation of 2.7 kJ/mol. This standard deviation, around 1% of the mean, is regarded as a particularly low value. To get a picture of the uncertainties of the activation energy in the non-isothermal kinetics, a round-robin study can be considered.[32] In that work a single, well-defined cellulose was studied, and the obtained standard deviations, 8 and 10 kJ/mol, were around 4% of the corresponding means.

A wide range of activation energies have been reported on the kinetics of CO_2 gasification of biomass chars, from 80 to 380 kJ/mol.[12,33] The present values are particularly close to the ones reported by Cozzani[34] for char from a refused derived fuel (221 kJ/mol), and by Wang el al.[22] for a spruce char prepared by a prolonged heating at 950°C (221 kJ/mol). The latter agreement is more relevant due to the similarity of the experimental and evaluation methods.

3.5. Pre-Exponential Factors and Reactivities. Table 3 shows that the $\log_{10} A$ values were obtained with a considerable standard deviation. As described in Sections 2.2 and 3.1, part of the 20°C/min experiments had different heating rates below the gasification domain. The experiments with 2°C/min heating rate in the pyrolysis domain gave nearly the same pre-exponential factors as the experiments which were heated at 20°C/min in the domain of pyrolysis. Here the corresponding $\log_{10} A$ values differed only in the third decimals. The untreated wood experiments with ca. 1400°C/min heating rate in the pyrolysis domain had higher $\log_{10} A$ values by 0.12 and 0.15 than their counterparts at regular heating. (Note that a higher A indicates higher reactivity at identical E and $f(\alpha)$. See also Table 2 in Section 3.1.) On the other hand, the fast heating in the pyrolysis domain had negligible effect on the $\log_{10} A$ values for samples B275 and S275, in accordance with the data presented in Section 3.1.

The $\log_{10} A$ values of the modulated and CRR experiments were considerably lower than the corresponding values of the 20°C/min experiments: the average of the differences were -0.19 for the modulated experiments and -0.24 for the CRR experiments. Note that the mean dT/dt of the modulated experiments was 5°C/min while the mean dT/dt values of the CRR experiments varied between 2.4 and 4.5°C /min. To check the effect of the $\log_{10} A$ changes more closely, $-dm^{calc}/dt$ curves were simulated with the $\log_{10} A$ values of the 20°C/min experiments. The real $-dm^{obs}/dt$ curves of the modulated and CRR experiments occurred at considerably higher temperatures than the ones simulated that way. The average differences for the modulated and CRR experiments were 17 and 15°C, respectively. The highest $\log_{10} A$ difference was observed for sample B750, when $\log_{10} A$ was 7.44 at 20°C/min and 7.16 in the CRR experiment. In the latter case the mean heating rate in the domain of gasification was particularly low, 2.46°C/min. The highest mass loss rate in this CRR experiment was 1 µg/s in the domain of gasification, while the corresponding value of the 20°C/min experiment was 5 µg/s. If there was a heat or mass transfer problem, the opposite effect could have been expected: the gasification peak of the 20°C/min experiment should have moved then to a higher temperature. This

observation can be interpreted as a consequence of thermal annealing (thermal deactivation), which means the slow rearrangement of the char into more stable chemical structures at elevated temperatures with the loss of a low amount of volatiles.[35-37] The thermal annealing and the gasification reactions compete with each other in the TGA experiments on CO_2 gasification.[35] However, the rate of the gasification sharply increases with the temperature while the annealing remains a slow process in the temperature domain studied. The lower reactivity of chars B750 and S750 may also be due to annealing. The preparation of these chars included heating to 750°C, a holding time of 10 minutes, and cooling. Accordingly these chars spent more time in the temperature domain of 700-750°C than the rest of the samples.

In the kinetic treatment of the present paper, the reactivity differences are expressed by the pre-exponential factor, as explained above. The effect of the magnitude of A can easily be exemplified at linear heating when a small change of A results in a shift along the temperature axis without a noticeable change in the shape and width of the peak (provided that E and the parameters of $f(\alpha)$ do not change.) This is an old knowledge in the non-isothermal reaction kinetics, it follows directly from the Coats-Redfern equation.[38] As mentioned earlier, the earlier work of Wang et al.[22] employed similar experimental and evaluation methods to the present one. In that work, however, the chars were prepared by a prolonged heating at 950°C, accordingly no significant thermal annealing effects could be expected during the gasification, and identical kinetic parameters could therefore be employed for the experiments with different temperature programs.

3.6. About the Fit Quality. The fit quality is illustrated in Figures 4 and 5. The plots in Figures 4 and 5 indicate that the model approximates reasonably the main course of the gasification, but cannot follow such irregularities as the double peak top of the spruce samples. Note that a double peak top occurs for all spruce samples, as shown in Figure 2, and can probably be due to chemical or physical inhomogeneity of the chars formed from spruce.
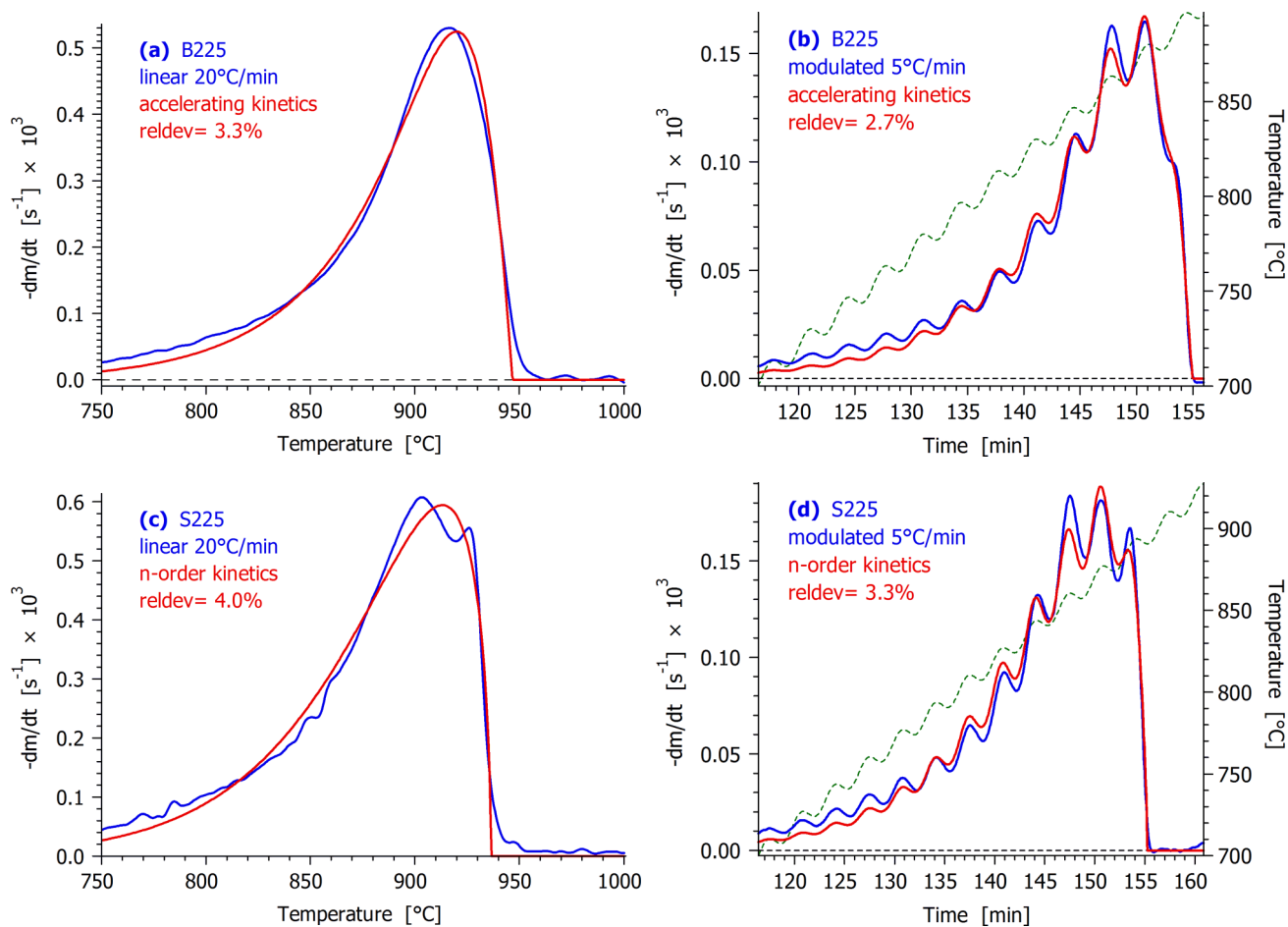
Figure 4. The fit quality illustrated by experiments with linear and modulated T(t) of the samples torrefied at 225°C. Notation: experimental –dm/dt curves (blue); their simulated counterparts (red); and the T(t) of the modulated experiments (green).

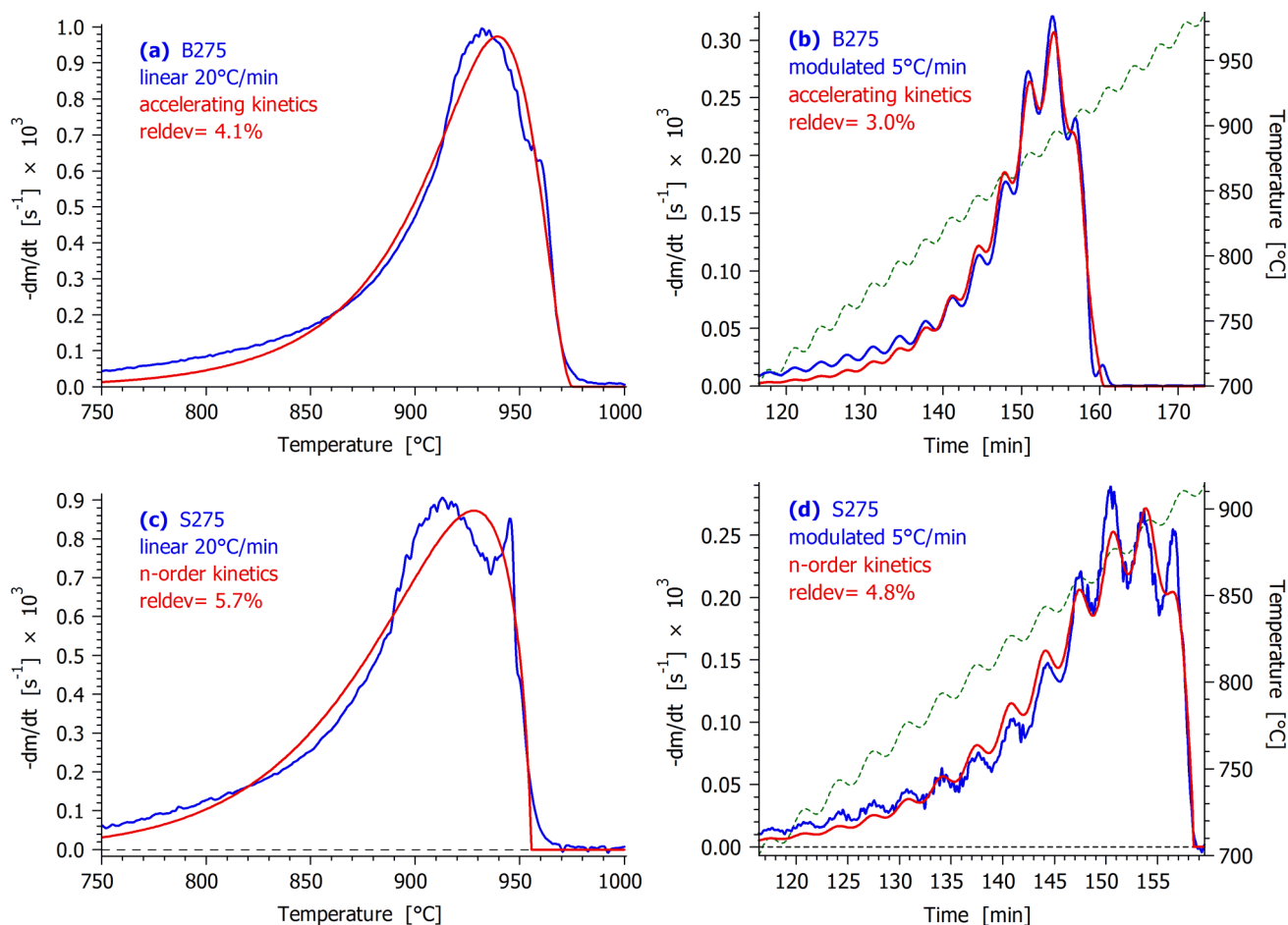**Figure 5.** The fit quality illustrated by experiments with linear and modulated T(t) of the samples torrefied at 275°C. Notation: see Figure 4.

4. CONCLUSIONS

(1) The CO_2 gasification of torrefied wood samples was examined. For comparison, the untreated raw materials and chars prepared at 750°C were also included in the study. The gasification temperature range was well separated from the pyrolysis (except a partial overlap with the slow char carbonization processes), as might have been expected. The pyrolysis heating rate (2, 20 and ~1400°C/min) in the TGA experiments had only negligible or moderate effects on the gasification reactivity of the formed chars. The gasification reactivity of the torrefied samples was more or less lower than that of the untreated woods. This observation was interpreted as the effect of secondary char forming reactions from tars when, during the torrefaction, the tars were swept away less efficiently from the larger samples used to produce the torrefied samples than from the smaller samples used in the TGA experiments.

(2) The kinetic evaluation of the gasification was based on experiments with linear, modulated and CRR temperature programs. Various groups of experiments were evaluated together, under various hypotheses on the dependence of the reaction rate on the reacted fractions, $f(\alpha)$. Nevertheless the obtained activation energy

values were close to each other, and scattered in a rather narrow interval. The mean of the activation energies obtained in the different evaluations were 124kJ/mol with a standard deviation below 3kJ/mol.

(3) When the experiments of a given sample were evaluated separately from the experiments of the other samples, the $f(\alpha)$ functions obtained for the spruce samples were monotonically decreasing, while the f(α) functions of the untreated and torrefied birch samples had a maximum at α=0.4 – 0.45.

(4) The experiments carried out at different temperature programs could not be described by the same kinetic parameters because the extent of the thermal annealing was higher during the temperature programs with slower heating. The different extent of the thermal annealing was expressed by different pre-exponential factors, while E and the parameter(s) of the $f(\alpha)$ function had identical values for the experiments on a given sample.

(5) In another evaluation the gasification of the samples derived from the same wood were described together with identical E and $f(\alpha)$. Here both the reactivity differences between the samples and the different extent of the thermal annealing were expressed by pre-exponential factors differing from experiment to experiment. In that case the $f(\alpha)$ obtained for the birch samples of the study had a maximum at α=0.38, and E was 225kJ/mol. The common $f(\alpha)$ obtained for the spruce samples was monotonously decreasing and could be described by n-order kinetics with n=0.38. Here E was 223kJ/mol, which is remarkably close to the value obtained for the birch samples.

ASSOCIATED CONTENT

Supporting Information

The effect of the pyrolysis heating rate on the gasification and the repeatability of the experiments are illustrated by figures. This information is available free of charge via the Internet at http://pubs.acs.org/.

AUTHOR INFORMATION

Corresponding Author

* To whom correspondence should be addressed. E-mail: varhegyi.gabor@t-online.hu, Tel. +36 1 2461894.

NOMENCLATURE

α = reacted fraction in the domain of gasification (dimensionless)

A = pre-exponential factor (s^{-1})

CRR = temperature programs that ensure a limited reaction rate during an experiment

E = activation energy (kJ/mol)

f = empirical function (equations 7 – 9) expressing the change of the reactivity as the reactions proceed (dimensionless)

h_k = height of an experimental $-dm/dt$ curve (s^{-1})

m = the mass of the sample normalized by the initial dry sample mass (dimensionless)

n = reaction order (dimensionless)

of = objective function minimized in the least squares evaluation (dimensionless)

N = number of experiments evaluated together by the method of least squares

N_k = number of evaluated data on the kth experimental curve

R = gas constant (8.3143×10^{-3} kJ mol^{-1} K^{-1})

$reldev$ = the deviation between the observed and calculated data expressed as per cent of the corresponding peak height

$reldev_N$ = root mean square of the $reldev$ values of N experiments

t = time (s)

T = temperature (°C, K)

T_{half} = temperature of the half mass loss in the domain of gasification (°C)

z = formal parameter in eq 9 (dimensionless)

Subscripts:

i = digitized point on an experimental curve

j = pseudocomponent

k = experiment

REFERENCES

1. van der Stelt, M. J. C.; Gerhauser, H.; Kiel, J. H. A.; Ptasinski, K. J. Biomass upgrading by torrefaction for the production of biofuels: A review. *Biomass Bioenergy* **2011**, *35*, 3748-3762.

2. Chew, J. J.; Doshi, V. Recent advances in biomass pretreatment – Torrefaction fundamentals and technology. *Renew. Sustain. Energy Rev.* **2011,** *15*, 4212-4222.

3. Prins, M. J.; Ptasinski, K. J.; Janssen, F. J. J. G. Torrefaction of wood. *J. Anal. Appl. Pyrolysis* **2006,** *77*, 35-40.

4. Marcilla, A.; Conesa, J.A.; Asensio, M.; García-García, S.M. Thermal treatment and foaming of chars obtained from almond shells: Kinetic study. *Fuel* **2000**, *79*, 829-836.

5. Cagnon, B.; Py, X.; Guillot, A.; Stoeckli, F.; Chambat, G. Contributions of hemicellulose, cellulose and lignin to the mass and the porous properties of chars and steam activated carbons from various lignocellulosic precursors. *Biores. Technol.* **2009**, *100*, 292-298.

6. Rousset, P.; Davrieux, F.; Macedo, L.; Perré, P. Characterisation of the torrefaction of beech wood using NIRS: Combined effects of temperature and duration. *Biomass Bioenergy* **2011,** 35, 1219-1226.

7. Melkior, T.; Jacob, S.; Gerbaud, G.; Hediger, S.; Le Pape, L.; Bonnefois, L.; Bardet, M. NMR analysis of the transformation of wood constituents by torrefaction. *Fuel* **2012,** 92, (1), 271-280.

8. Chen, W.-H.; Kuo, P.-C., Torrefaction and co-torrefaction characterization of hemicellulose, cellulose and lignin as well as torrefaction of some basic constituents in biomass. *Energy* **2011,** 36, (2), 803-811.

9. Tapasvi, D.; Khalil, R.; Várhegyi, G.; Tran, K.-Q.; Grønli, M.; Skreiberg, Ø.: Thermal decomposition kinetics of woods with an emphasis on torrefaction. *Energy Fuels* **2013**, *27,* 6134-6145.

10. Prins, M. J.; Ptasinski, K. J.; Janssen, F. J. J. G. More efficient biomass gasification via torrefaction. Energy **2006**, *31*, 3458–3470.

11. Svoboda, K.; Pohořelý, M.; Hartman, M.; Martinec, J. Pretreatment and feeding of biomass for pressurized entrained flow gasification. *Fuel Process. Technol.* **2009**, *90*, 629-635.

12. Di Blasi, C. Combustion and gasification rates of lignocellulosic chars. *Prog. Energy Combust. Sci.* **2009,** *35*, 121-140.

13. Lahijani, P.; Zainal, Z. A.; Mohammadi, M.; Mohamed, A. R. Conversion of the greenhouse gas CO2 to the fuel gas CO via the Boudouard reaction: A review. *Renew. Sustain. Energy Rev.* **2015**, *41*, 615–632.

14. Irfan, M. F.; Usman, M. R.; Kusakabe, K. Coal gasification in CO_2 atmosphere and its kinetics since 1948: A brief review. *Energy* **2011**, *36*, 12-40.

15. Ibrahim, R. H. H.; Darvell, L., I.; Jones, J. M.; Williams, A. Physicochemical characterisation of torrefied biomass. *J. Anal. Appl. Pyrol.* **2013**, *103*, 21-30.

16. Marcilla, A.; García-García, S.; Asensio, M.; Conesa, J.A. Influence of thermal treatment regime on the density and reactivity of activated carbons from almond shells. *Carbon* **2000**, *38*, 429-440.

17. Fisher, E. M.; Dupont, C.; Darvell, L. I.; Commandre, J. M.; Saddawi, A.; Jones, J. M.; Grateau, M.; Nocquet, T.; Salvador, S. Combustion and gasification characteristics of chars from raw and torrefied biomass. *Biores. Technol.* **2012**, *119*, 157-165.

18. Xue, G.; Kwapinska, M.; Kwapinski, W.; M. Czajka, K. M.; Kennedy, J.; Leahy, J. J. Impact of torrefaction on properties of Miscanthus × giganteus relevant to gasification. *Fuel* **2014**, *121*, 189-197.

19. Tapasvi, D.; Khalil, R. A.; Skreiberg, Ø.; Tran, K.-Q.; Gronli, M. G. Torrefaction of Norwegian birch and spruce – An experimental study using macro-TGA. *Energy Fuels* **2012**, *26,* 5232−5240.

20. Tapasvi, D.; Khalil, R.; Várhegyi, G.; Skreiberg, Ø.; Tran, K.-Q.; Grønli, M.: Kinetic behavior of torrefied biomass in an oxidative environment. *Energy Fuels,* **2013**, *27,* 1050-1060.

21. High resolution thermogravemetric analysis - A new technique for obtaining superior analytical results. TA Instruments report TA-023. Available at: http://www.tainstruments.co.jp/application/pdf/Thermal_Library/Applications_Briefs/TA023.PDF

22. Wang, L.; Sandquist, J.; Várhegyi, G.; Matas Güell, B.: CO_2 Gasification of chars prepared from wood and forest residue. A kinetic study. *Energy Fuels,* **2013**, *27,* 6098-6107.

23. Várhegyi, G.; Sebestyén, Z.; Czégény, Z.; Lezsovits, F.; Könczöl, S.: Combustion kinetics of biomass materials in the kinetic regime. *Energy Fuels,* **2012**, *26*, 1323-1335.

24. Várhegyi, G.; Chen, H.; Godoy, S.: Thermal decomposition of wheat, oat, barley and *Brassica carinata* straws. A kinetic study. *Energy Fuels* **2009**, *23*, 646-652.

25. Várhegyi, G.; Szabó, P.; Mok W. S. L., Antal, M. J., Jr.: Kinetics of the thermal decomposition of cellulose in sealed vessels at elevated pressures. Effects of the presence of water on the reaction mechanism. *J. Anal. Appl. Pyrolysis* **1993**, *26*, 159-174.

26. Antal, M.J.; Grønli, M. The art, science, and technology of charcoal production. *Ind. Eng. Chem. Res.* **2003**, *42*, 1619-1640.

27. Wang, L.; Skreiberg, Ø.; Gronli, M.; Specht, G. P.; Antal, M. J. Is elevated pressure required to achieve a high fixed-carbon yield of charcoal from biomass? Part 2: The importance of particle size. *Energy Fuels* **2013**, *27*, 2146-2156.

28. Bhatia; S. K; Perlmutter, D. D. A random pore model for fluid–solid reactions: I. Isothermal kinetic control. *AIChE J.* **1980**, *26*, 379-386.

29. Gavalas, G. R. A random capillary model with application to char gasification at chemically controlled rates. *AIChE J.* **1980**, *26*, 577-585.

30. Ballal, G.; Zygourakis, K. Evolution of pore surface-area during noncatalytic gas solid reactions .1. Model development. *Ind. Eng. Chem. Res.* **1987**, 26, 911-921.

31. Várhegyi, G.; Szabó, P.; Jakab, E.; Till, F.; Richard J-R. Mathematical modeling of char reactivity in Ar-O_2 and CO_2-O_2 mixtures. *Energy Fuels* **1996**, *10*, 1208-1214.

32. Grønli, M.; Antal, M. J., Jr.; Várhegyi, G. A round-robin study of cellulose pyrolysis kinetics by thermogravimetry. *Ind. Eng. Chem. Res.* **1999**, *38* , 2238-2244.

33. Vamvuka, D.; Karouki, E.; Sfakiotakis S. Gasification of waste biomass chars by carbon dioxide via thermogravimetry. Part I: Effect of mineral matter. *Fuel* **2011**, *90*, 1120-1127.

34. Cozzani, V. Reactivity in oxygen and carbon dioxide of char formed in the pyrolysis of refuse-derived fuel. *Ind. Eng. Chem. Res.* **2000**, *39*, 864-872.

35. Senneca, O.; Russo, P.; Salatino, P.; Masi, S. The relevance of thermal annealing to the evolution of coal char gasification reactivity. *Carbon* **1997**, *35*, 141-151.

36. Zolin, A.; Jensen, A.; Dam-Johansen, K.; Jensen, L. S. Influence of experimental protocol on activation energy in char gasification: the effect of thermal annealing. *Fuel* **2001**, *80*, 1029-1032.

37. Yip, K.; Xu, M.; Li, C-Z.; Jiang, S. P.; Wu, H. Biochar as a fuel: 3. Mechanistic understanding on biochar thermal annealing at mild temperatures and its effect on biochar reactivity. *Energy Fuels*, **2011**, *25*, 406-414.

38. Coats, A. W.; Redfern, J. P. Kinetic parameters from thermogravimetric data. *Nature* **1964**, *201,* 68-69.